Characterisation of convective regimes over the British Isles

It is advisable to refer to the publisher's version if you intend to cite from the work.

To link to this article DOI: http://dx.doi.org/10.1002/qj.2758

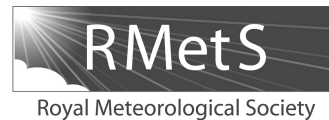## www.reading.ac.uk/centaur

CentAUR

RMetS

Royal Meteorological Society

Characterisation of convective regimes over the British Isles

David L. A. Flack,[a]* Robert S. Plant,[a] Suzanne L. Gray,[a] Humphrey W. Lean,[b]† Christian Keil[c]
and George C. Craig[c]

[a]*Department of Meteorology, University of Reading, UK*
[b]*MetOffice@Reading, University of Reading, UK*
[c]*Meteorologisches Institut, Ludwig-Maximilians-Universität München, Germany*

*Correspondence to: D. L. A. Flack, Department of Meteorology, University of Reading, Earley Gate, PO Box 243, Reading
RG6 6BB, UK. E-mail: d.l.a.flack@pgr.reading.ac.uk*
†The contribution of H. W. Lean is published with the permission of the Controller of HMSO and the Queen's Printer for Scotland

Convection-permitting modelling has led to a step change in forecasting convective events. However, convection occurs within different regimes which exhibit different forecast behaviour. A convective adjustment timescale can be used to distinguish between these regimes and examine their associated predictability. The convective adjustment timescale is calculated from radiosonde ascents and found to be consistent with that derived from convection-permitting model forecasts. The model-derived convective adjustment timescale is then examined for three summers in the British Isles to determine characteristics of the convective regimes for this maritime region. Convection in the British Isles is predominantly in convective quasi-equilibrium, with 85% of convection having a timescale less than or equal to 3 h. This percentage varies spatially with more non-equilibrium events occurring in the south and southwest. The convective adjustment timescale exhibits a diurnal cycle over land. The non-equilibrium regime occurs more frequently at mid-range wind speeds and with winds from southerly to westerly sectors. Most non-equilibrium convective events in the British Isles are initiated near large coastal orographic gradients or on the European continent. Thus, the convective adjustment timescale is greatest when the location being examined is immediately downstream of large orographic gradients and decreases with distance from the convective initiation region. The dominance of convective quasi-equilibrium conditions over the British Isles argues for the use of large-member ensembles in probabilistic forecasts for this region.

Key Words: convection; convective adjustment timescale; convective quasi-equilibrium; non-equilibrium convection; MetUM

Received 13 August 2015; Revised 29 December 2015; Accepted 29 January 2016; Published online in Wiley Online Library

1. Introduction

Forecasting convective events is an important problem, not least because of the socio-economic impacts of flash floods which may result from intense localised precipitation produced by convection (Hand *et al.*, 2004). Convection-permitting models are now being run operationally by several weather forecasting centres (e.g. Baldauf *et al.*, 2011; Seity *et al.*, 2011; Tang *et al.*, 2013, for Météo-France, Deutscher Wetterdienst (DWD) and Met Office, respectively) and have led to a step change in forecasts of convective precipitation (e.g. Lean *et al.*, 2008). However, deterministically forecasting convective events will always remain a challenging problem due to their low intrinsic predictability (Lorenz, 1969). Probabilistic forecasts, generated through the use of well-spread convection-permitting ensembles, can provide

practical information on the predictability of these events (e.g. Done *et al.*, 2012).

Done *et al.* (2006, 2012) and Keil and Craig (2011) have demonstrated that convective predictability within models can exhibit very different characteristics depending on the environmental conditions in which the event occurs. These differing environmental conditions are often thought of as distinct weather regimes. Understanding these regimes and their frequency of occurrence for different locations is therefore of particular importance if convective forecasts are to improve beyond just increasing the model resolution.

Convection is classically considered to occur within two distinct regimes: convective quasi-equilibrium and non-equilibrium (e.g. Emanuel, 1994). The concept of convective quasi-equilibrium originated from the closure problem for convection schemes and

was proposed by Arakawa and Schubert (1974). A modern review of the concept can be found in Yano and Plant (2012). Convective quasi-equilibrium arises when the budget equation for some measure of convective instability is in a state of approximate balance, such that its production rate on large (synoptic) scales is balanced by its release on small (convective) scales. Thus, the overall time tendency of the measure is close to zero. The concept was originally formulated in terms of the cloud work-function of Arakawa and Schubert (1974), but other measures, most notably the Convective Available Potential Energy (CAPE) which is a special case of the cloud work-function for non-entraining parcel ascent, have often been preferred. Convective quasi-equilibrium events within the midlatitudes can often be linked with smaller CAPE values than non-equilibrium convection (Done *et al.*, 2006). The smaller CAPE implies limited instability in the atmosphere such that persistent, but relatively modest, convective activity may be enough to return the atmosphere towards neutral conditions.

Non-equilibrium convection, also referred to as 'triggered convection' (Emanuel, 1994), occurs when CAPE builds up over a period of time, and so can result in large values of CAPE. For conditions to allow a build-up of CAPE, some inhibiting factor is required, such as a layer of stable air. This is often indicated by the presence of Convective Inhibition (CIN). Convection will initiate if the CIN can be overcome, and may lead to the rapid formation of strong convection. This type of event often occurs over continents in the early spring or summer (Weckwerth and Parsons, 2006) due to large areas exposed to insolation, but is perhaps less common for islands such as the UK (Bennett *et al.*, 2006).

To investigate more systematically how the behaviour of convection depends upon the prevailing regime, it is necessary to have some quantitative method for distinguishing between the regimes. Done *et al.* (2006) proposed that a convective adjustment timescale, τ_c, was a suitable diagnostic for the purpose, defining it as the ratio between the CAPE and its rate of change at convective scales, i.e.

$$\tau_c = \frac{\text{CAPE}}{|\partial \text{CAPE}/\partial t|_{\text{CS}}},$$

where the subscript CS refers to convective scales. The denominator is not in a convenient form for calculation from observational data or standard model output. However, it can be estimated from the precipitation rate since this provides an indication of the column latent heating associated with convective activity. Of course, CAPE can be released through various mechanisms of which diabatic heating is one possibility (Arakawa and Schubert, 1974; Emanuel, 1994). Nonetheless, the estimate may be expected to be reasonable in many convective situations and leads to a simple and practical formula for the convective adjustment timescale (Done *et al.*, 2006):

$$\tau_c = \frac{1}{2} \frac{c_p \rho_0 T_0}{L_v g} \frac{\text{CAPE}}{P_{\text{rate}}}, \qquad (1)$$

where c_p is the specific heat capacity of air at constant pressure, ρ_0 and T_0 are a reference density and temperature respectively, L_v is the latent heat of vaporisation, g the acceleration due to gravity and P_{rate} the precipitation rate. The last of these is likely best estimated as an accumulation over time converted into a precipitation rate. The factor of one half was introduced by Molini *et al.* (2011) as a simple attempt to take account of some neglected aspects of the calculation such as water-loading effects and boundary-layer modifications, the neglect of which would tend to produce an over-estimation of the convective adjustment timescale (Keil and Craig, 2011).

The convective adjustment timescale has been used to separate regimes and so contrast the predictability of convection. Done *et al.* (2006, 2012) showed that the predictability of both the location and intensity of convective events depends upon the regime, with convective quasi-equilibrium events having a predictable area-averaged precipitation but low predictability in terms of location, whilst the opposite was found for non-equilibrium events. This idea was developed by Keil and Craig (2011) who showed that ensemble members, generated in different ways, all perform similarly in situations where the large-scale flow dominates; this situation is typical of convective quasi-equilibrium. It has also been shown (Keil *et al.*, 2014) that model physics perturbations provide a greater contribution to the spread in precipitation rate in cases of weak synoptic forcing (i.e. the non-equilibrium regime).

The convective adjustment timescale has also proved valuable for other purposes. Craig *et al.* (2012) showed that latent heat nudging of radar data into a COSMO-DE ensemble (Consortium for Small Scale Modelling–domain over Germany) had a large impact on convection in the non-equilibrium regime as the extra data improved the intensity estimates. However, if the convection was in quasi-equilibrium then the impact of data assimilation decayed rapidly (within a couple of hours) as the convection rapidly readjusted to its synoptic environment. More recent studies using the convective adjustment timescale have focused on forecast blending (i.e. combination of nowcasting and high-resolution forecasts in the short range) and the relationship with downscaled initial condition perturbations for convective-scale ensembles (Kober *et al.*, 2014; Kühnlein *et al.*, 2014) to further consider designs for short-range forecasts and convective-scale ensembles.

An important context for these (and our) investigations is provided by a climatological study of the convective adjustment timescale by Zimmer *et al.* (2011). This was based upon observations of CAPE and precipitation over Germany and categorised 66% of convective situations there as being consistent with convective quasi-equilibrium conditions, when a threshold of 12 h was considered. There was not a clean split in the regimes and it was suggested the regimes should be viewed as two extremes of a continuum, with the frequency distribution of the timescale appearing to follow a power law. The categorisation produced a slightly more even split in the summer months (June, July and August; JJA), compared to the split in the data from May to October, with 59% of the convection in JJA being in quasi-equilibrium (again with a threshold of 12 h). It seems entirely plausible that convection in other regions, such as the British Isles, may have a different split between the regimes. The coastline and topography of Britain are well known to have a strong impact on the initiation of convection, as reviewed by Bennett *et al.* (2006). The wind direction also has an influence on the convection influencing the British Isles; for example, a climatology of showers (Hand, 2005) showed that showers occurred in flow from the westerly sector most frequently, regardless of the season (Figure 3 in Hand, 2005).

In this study we construct a model climatology of the convective adjustment timescale for the British Isles, and focus on the frequency of the regimes, diurnal and spatial influences on the regimes across the British Isles and the dependence of convective regime occurrence on the large-scale wind direction. It is hypothesised that both the presence of coastlines and the wind direction will have an impact on climatological convection characteristics over the British Isles, given that it is often subject to convection that has initiated on the European continent. This may occur, for example, in 'Spanish plume' synoptic scenarios (Lewis and Gray, 2010). It is further hypothesised that a regional dependence will be found (Figure 1). The western coast of the mainland UK is likely to have more non-equilibrium situations than the eastern coast due to the relative steepness of the orography. Forced ascent in this region may help to overcome any CIN present and the flow within complex terrain may lead to the development of convergence lines. The coastline itself is also hypothesised to contribute to regime characteristics through associated convergence lines, a good example being the initiation
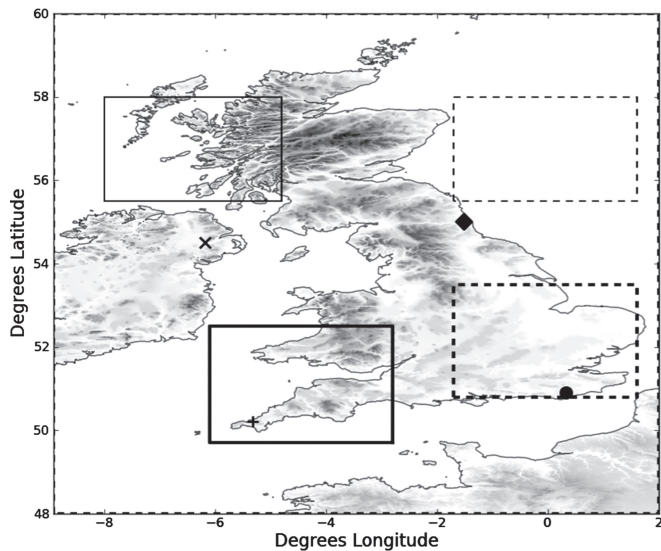
Figure 1. A map of the British Isles. The large dashed region represents the area that was coarse-grained in the calculation of the timescale. The smaller boxes represent averaging domains for specific regions of the British Isles. The solid box represents the west Scottish coast, the solid bold box represents southwest England and south Wales, the dashed box is the North Sea region and the bold dashed box is southeast England. The symbols represent the location of radiosonde stations: Camborne ($+$), Castor Bay ($\times$), Herstmonceux ($\bullet$) and Albemarle ($\diamond$).

of the flash flooding event in Boscastle 2004 (Golding *et al.*, 2005; Burt, 2005; Warren *et al.*, 2014). Further understanding of these regimes, and other factors that they are associated with, may lead to further improvements in forecasts, not just from a deterministic or ensemble perspective but also from an adaptive forecasting perspective.

This article is organised as follows. The model data used are described in section 2, followed by details of the method chosen for determining the timescale. Results obtained from the model data are compared against available observations in section 3. The main results from the model climatology are presented and discussed in section 4, which focuses on the relative frequency of the regimes, the spatial and temporal scales of the timescale and its relationship with the large-scale flow. A summary and conclusions are provided in section 5.

2. Data and methods

2.1. Model output

The Met Office Unified Model (MetUM) is a non-hydrostatic, semi-implicit, semi-Lagrangian model (Davies *et al.*, 2005). It uses the surface layer scheme of Best *et al.* (2011), the microphysics scheme of Wilson and Ballard (1999), the radiation scheme of Edwards and Slingo (1996) and the boundary-layer scheme of Lock *et al.* (2000). The configuration used in this study was the United Kingdom Variable resolution (UKV) which has been the operational UK model since 2009. The UKV configuration represents convection explicitly rather than through a convection scheme as it has a grid length of 1.5 km in its interior domain (an early convection-permitting version of the MetUM is discussed by Lean *et al.*, 2008). At the edges of the UKV domain, the grid length is tapered from 4 to 1.5 km (Tang *et al.*, 2013) – this variable resolution reduces problems with spin-up of convection at the boundaries of the model. However, the interior model grid length of 1.5 km is not fine enough to fully resolve convection (Craig and Dörnbrack, 2008; Stein *et al.*, 2015), so it is classed as a convection-permitting model. There are 70 levels in the vertical with the highest at 40 km (Hanley *et al.*, 2014). The Met Office operational configuration uses 3D variational (3D-Var) data assimilation with 3-h cycling. This model is directly one-way

nested into the global configuration (grid length 25 km) of the MetUM.

The operational output from the interior domain of the UKV was coarse-grained to a 60 km grid to reduce computational expense and to extend the study for more than a season. A grid of 60 km was chosen to allow comparison with the timescale calculated from a coarser-resolution convection-parametrizing model configuration (the North Atlantic European domain (NAE) of the MetUM). The NAE has a horizontal grid length of 12 km, which would be expected to resolve features reasonably well on a scale of 60 km. It was found that the convection-permitting model yields better estimates of the timescale than the NAE operational output due to improved CAPE values (not shown). The improvement is thought to come from the explicit representation of convection increasing the CAPE values compared to the convection parametrization scheme which did not allow enough CAPE.

The data used for the model climatology were the operational forecasts initiated at 0300 UTC for JJA 2012−2014. The 0300 UTC forecasts were used as they were most likely to capture the entire life-cycle of a convective event on any particular day in the period examined. Throughout this study the model output for 24 h periods from 0900 to 0900 UTC (T + 6 h to T + 30 h) has been used as an optimal balance between reducing errors associated with spin-up and with longer lead times. Three summer seasons were used to allow robust conclusions to be drawn given the frequency of convective events in the British Isles. The summers chosen cover a wet (2012), dry (2013) and average (2014) summer, with 157%, 78% and 107% of climatological precipitation respectively (Met Office, 2012b, 2013, 2014). Although these summers had different total precipitation accumulations, the timescale statistics behind each year were consistent, with the same distribution present in Figure 4(c) below occurring in all of the years considered. The length of the climatology is limited by the period that the UKV has been operational, and current computing practicalities.

Both CAPE and the precipitation accumulations were derived from the model. CAPE was calculated as the maximum CAPE lifted from the first 30 levels from every third level, representing surface pressure to approximately 850 hPa,

$$\text{CAPE} = \int_{p_{\text{LNB}}}^{p_{\text{lift}}} R \left(T_{\text{p}} - T_{\text{a}} \right) \mathrm{d}(\ln p),$$

where p_{lift} is the pressure the air parcel is lifted from, p_{LNB} is pressure at the level of neutral buoyancy, R is the specific gas constant of dry air, T_{p} and T_{a} are parcel and ambient temperatures and p is pressure. The CAPE was calculated at each hour and averaged over a 3 h period. The precipitation values were 3 h accumulations converted into a precipitation rate to keep unit consistency.

2.2. Observational data

The CAPE was also calculated from radiosonde ascents at four stations within the British Isles (marked on Figure 1) for summer 2013. The ascents used at Camborne were at 0000 and 1200 UTC, whereas the ascents for Castor Bay, Herstmonceux and Albemarle were at 0000 UTC (with data obtained from the British Atmospheric Data Centre, BADC; Met Office, 2006). The relative coarseness of the location of radiosonde stations is the reason why model output is primarily used in this article.

Consistency in calculation method is required so that a fair comparison can be made between the observational data and model output used. Therefore the observed CAPE is calculated as the maximum CAPE lifted from the first 164 data levels from the radiosonde (surface to approximately 850 hPa). However, as the radiosonde data have a higher vertical resolution than the model, the radiosonde data have been arithmetically averaged over every five levels and parcels were lifted from every third level

of this averaged profile. Observational data have been used for one year due to limited available data for 2012 and 2014. However, consistency in the model and the data available from those years indicated similar results to those discussed in section 3.

Precipitation data from the Met Office Land and Sea observations dataset (MIDAS; also obtained from the BADC; Met Office, 2012a) for gauges at the radiosonde launch sites were used. Accumulations of hourly precipitation were used to compare the precipitation for model and UKV data, and 3 h accumulations were used to compare observation- and model-derived convective adjustment timescales.

2.3. Calculation of the convective adjustment timescale

As with previous studies considering the convective adjustment timescale (Done *et al.*, 2006; Molini *et al.*, 2011; Keil and Craig, 2011; Zimmer *et al.*, 2011; Craig *et al.*, 2012; Kober *et al.*, 2014; Kühnlein *et al.*, 2014; Keil *et al.*, 2014) it was found helpful to specify a threshold in the timescale to separate between the different regimes. The value of the threshold has varied in previous studies within the range 3 h (area averaged; Keil *et al.*, 2014) to 12 h (coarsened scale; Kober *et al.*, 2014), with most using 6 h (Molini *et al.*, 2011; Keil and Craig, 2011; Craig *et al.*, 2012; Kühnlein *et al.*, 2014). Done *et al.* (2006) also used a threshold of 6 h. However, this was before the factor of one half had been introduced in the equation for the convective adjustment timescale so this threshold is equivalent to 3 h as calculated using Eq. (1).

Zimmer *et al.* (2011) concluded that a threshold within the region 3–12 h should distinguish clearly between the different regimes. A threshold of 3 h is used here; values above this threshold are considered to be non-equilibrium convection and values below are considered to be quasi-equilibrium convection. The timescale threshold chosen is stated here but justified *a posteriori* based on the results presented.

Previous studies have calculated the convective adjustment timescale using a number of methods for spatially and temporally smoothing the raw CAPE and precipitation data (Done *et al.*, 2006; Molini *et al.*, 2011; Keil and Craig, 2011). These methods include averaging over points where it is raining (Molini *et al.*, 2011) and using a Gaussian kernel to smooth the CAPE and precipitation fields (Keil and Craig, 2011). The methods used in earlier studies were tested alongside other variants to determine if the regime separation was sensitive to the method used for smoothing. The results were also compared against the following set of criteria that was obtained from theory and previous studies:

- the timescale should be representative of an ensemble of clouds (Craig *et al.*, 2012) and should not be influenced by variability on scales smaller than the spacing between the convective clouds (Done *et al.*, 2006);
- the timescale should be temporally smooth so it does not jump erratically between regimes (Keil and Craig, 2011);
- the timescale should be spatially smooth and indicate localised features (Keil and Craig, 2011).

The derived convective adjustment timescales implied similar regime separation for all the smoothing methods trialled, provided that precipitation accumulations were used instead of instantaneous precipitation rates. There was greater variation in the derived convective adjustment timescales for different smoothing methods when the calculations were performed on data from the model configuration using a convection parametrization scheme (the NAE) compared to data from a model configuration that treated convection explicitly (the operational UKV). The MetUM uses a convection scheme with a convective quasi-equilibrium-type closure (Gregory and Rowntree, 1990) and, based on the derived convective adjustment timescale, all the cases used in the sensitivity tests were classed as convective quasi-equilibrium events when instantaneous precipitation rates from the NAE configuration

were used. This helps to motivate the choice of the UKV model configuration for the model-derived convective adjustment timescales here.

From the sensitivity testing, it was determined that the smoothing method of Keil and Craig (2011) would be used as it met all of the above criteria. A Gaussian kernel of half-width 60 km is applied to the coarse-grained CAPE and precipitation fields, and the convective adjustment timescale is calculated every 3 h. A threshold of $0.2 \, \mathrm{mm \, h^{-1}}$ is applied to the precipitation accumulations (after conversion to a precipitation rate and the Gaussian kernel has been applied) so that the timescale does not tend to infinity for very light (and likely non-convective) precipitation events or dry events. This threshold is smaller than that used in any previous study referenced here because of the coarse-graining applied to the UKV output. The precipitation threshold removes all but the top 17% of accumulations to reduce the chance of any stratiform rain being included in the calculation. Throughout this study, unless otherwise specified, CAPE values of zero and precipitation values below the threshold were included in the data being smoothed, but undefined convective adjustment timescales resulting from the smoothed data are not included.

As described in section 2.1, the precipitation and CAPE fields are coarse-grained prior to their use to calculate the convective adjustment timescale. Coarse-graining retained the large-scale structure in the precipitation and CAPE fields from the 1.5 km grid-length model and calculations of the timescale produced comparable results between the operational and coarse-grained UKV output in terms of the regime classification inferred using a threshold of 3 h. Figure 2 shows examples of the convective adjustment timescale calculated for two different cases. Figure 2(a, c, e) are for 2 August 2013, which was an intensive observing period of the Convective Precipitation Experiment (COPE; Leon *et al.*, 2015) field campaign that occurred in July and August 2013, and Figure 2(b, d, f) are from 20 April 2012, which was an intensive observing period of the Dynamical and Microphysical Evolution of Convective Storms (DYMECS; Stein *et al.*, 2015) field campaign. Figure 2 shows τ_c for the two cases calculated directly from the UKV interior domain data (at 1.5 km horizontal grid spacing) and from that coarse-grained to 60 km. Radar composites (from the BADC; Met Office, 2003) are also shown for the two days, to give a sense of the different convection occurring on each day. Figure 2 shows that the regime split is similar for UKV data and the coarse-grained UKV data, with convection being placed in the non-equilibrium regime for 2 August 2013. There is an average timescale of 11.5 h at 1.5 km grid spacing and 8.7 h with coarse-grained data. The second case, 20 April 2012, is a little more complex to consider. The timescale, as a domain average, at 1.5 km grid spacing is 3.6 h. This value goes over the threshold of 3 h because of a small area of convection in the domain with a timescale greater than 12 h. If this region is removed, the domain-average timescale reduces to 0.24 h. Hence, most of the convection occurring is in quasi-equilibrium. When the coarse-graining is applied to this case, the average value is 1.9 h, further implying that convection was in quasi-equilibrium.

3. Comparison of observations against model output

There are several caveats in using model data for a climatology. There are a number of known biases in the representation of convective precipitation in the UKV (in common with other kilometre-scale models). These biases are

(i) that the peak precipitation rate in the middle of shower cells is too intense, leading to large local precipitation accumulations (Stein *et al.*, 2015);
(ii) the convective cells are too circular, with some of the surrounding light rain (observed on radars) being absent in the model (Lean *et al.*, 2008; Stein *et al.*, 2015);
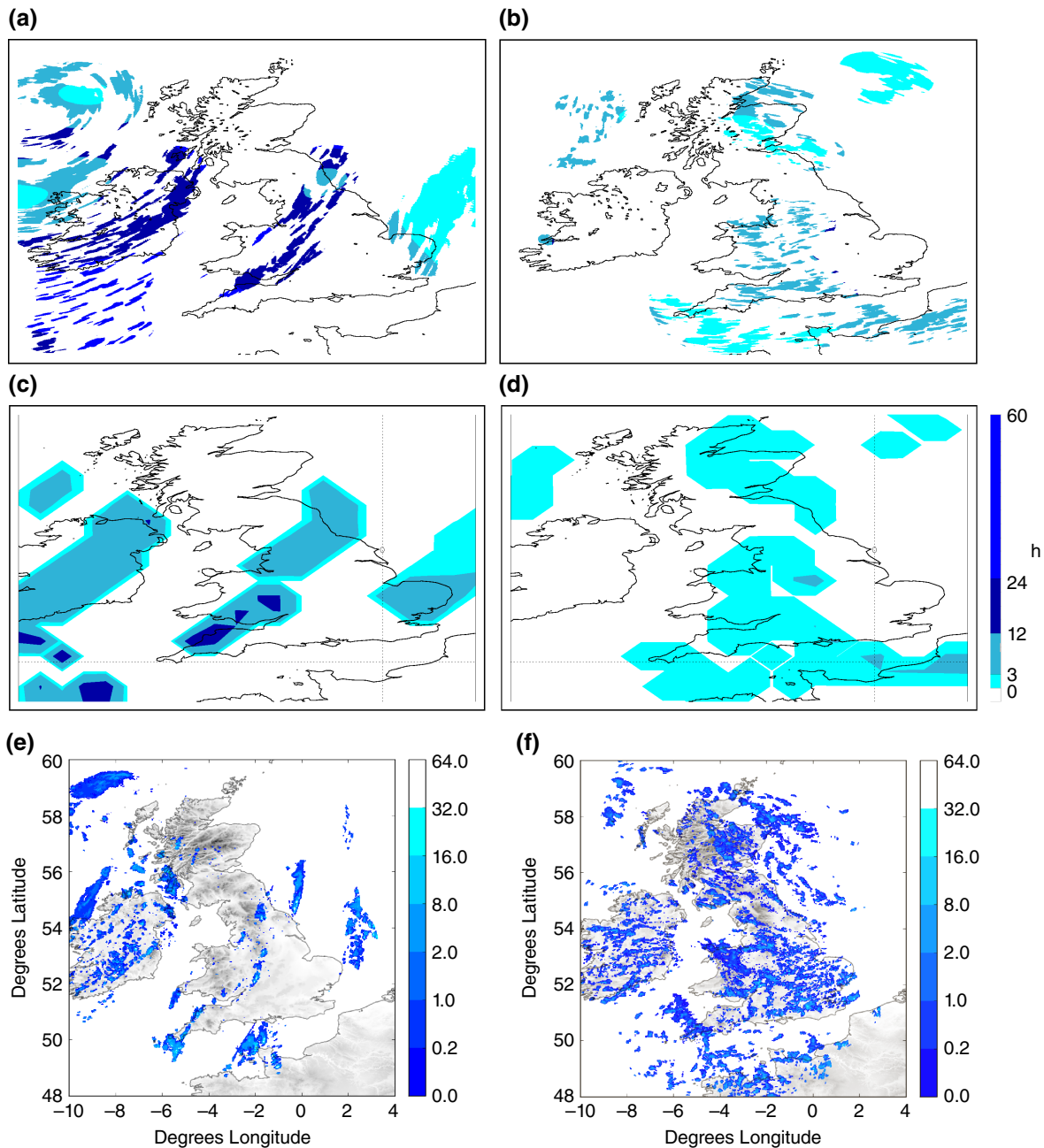
Figure 2. The convective adjustment timescale calculated for (a, c, e) 1500 UTC on 2 August 2013 and (b, d, f) 1100 UTC on 20 April 2012, using (a, b) the UKV model output at 1.5 km, and (c, d) the UKV model output coarse-grained to a grid length of 60 km. The colour scale to the right of (d) refers to all previous panels, with white representing an undefined timescale. Radar composite maps of the British Isles show precipitation rates (mm h^{-1}) for the two days at (e) 1525 UTC and (f) 1155 UTC.

(iii) convective initiation is often delayed by around an hour (Lean *et al.*, 2008).

There are also problems with CAPE estimation from model data including insufficient vertical resolution leading to an underestimation of the CAPE, and CAPE often being retained too long before release by the model (Glinton, 2013). To see how such problems may influence the convective adjustment timescale climatology, we compare the model and observations for summer 2013.

To compare CAPE derived from the radiosonde ascent data with that derived from the model output, the coarse-grained output from the grid point closest to the sonde launch site was used for the model output. Using a coarse-grained field here is reasonable as CAPE is typically a smoothly varying field (relative to a typical precipitation field) and so is unlikely to change rapidly with distance. To compare the modelled precipitation with the point rain-gauge observations, the precipitation at the closest UKV model grid point was chosen due to the uneven

distribution of rain gauges over the coarse-graining scale and the high spatial variability of convective precipitation. Consequently, comparison of the precipitation will be subject to the double penalty problem caused by the wrong positioning of a convective cell – a problem with precipitation verification in all convection-permitting models.

Figure 3(a) indicates that the model performs reasonably well in its CAPE estimation, with a correlation of 0.66 to the observations. Occasionally the model has larger CAPE than observed, especially for small CAPE values (the points in Figure 3(a) where the observed values are less than 10 but observed values are over 50 J kg^{-1}). However, it is worth stressing that, whilst the values depart from the one-to-one line for the smallest values of CAPE (Figure 3(a)), both model and observations usually agree that the CAPE should be low. The situations where there are large differences between the observed and model CAPE typically occur when the model retains CAPE compared to reality (Lean *et al.*, 2008), evidence for this is provided by a time series of CAPE (not shown). The delay is most likely linked to delayed
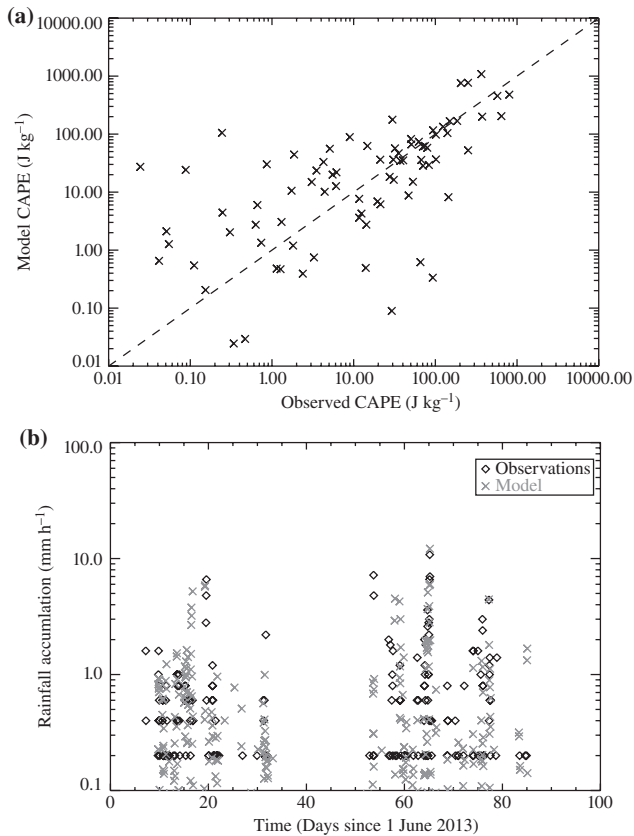
Figure 3. Model and observations comparisons showing (a) a scatter plot for the CAPE at Camborne for JJA 2013, showing all data except where either model or observed CAPE are zero, with a 1:1 line, and (b) a time series comparison of hourly precipitation accumulations at Camborne for JJA 2013, with observations in black and model in grey.

precipitation in convection-permitting models, and as such is a caveat of using model data, although the use of 3 h accumulations for the climatology should help to alleviate the impact of the delay. Consequently, there may be situations when the model convective adjustment timescale is longer than that calculated from observations.

The observed and modelled precipitation have not been rigorously compared for the purposes of this study. The key requirement is that it is precipitating at the right time, with similar accumulations. Figure 3(b) indicates that this is the case for the majority of the precipitation events, although there is a wet bias for this site which could result in a timescale being calculated that may have been undefined if using observational rain-gauge data. The results shown in Figure 3 are for Camborne. Figure 1 indicates locations of other radiosonde sites across the British Isles used for observational and model comparison. All of these sites, Albemarle, Herstmonceux and Castor Bay, give similar structure and timing of the peaks for the CAPE and the precipitation compared to Camborne (not shown). These results indicate that the model precipitation and CAPE fields are fit for the purpose of this study. A more rigorous verification of precipitation from a convection-permitting configuration of the MetUM has been performed by Mittermaier *et al.* (2013) and Mittermaier (2014). Combining the precipitation and CAPE fields together results in the convective adjustment timescale. Although there were relatively few convective events in summer 2013 (section 2.1), the model regime separation was very similar to that shown by the observations in all the locations examined (not shown). Although differences in the absolute value of the timescale exist, the regime separation is robust using the 3 h threshold chosen in section 2.3. Discrepancies occurred primarily when there were differences between the observed and modelled CAPE field or an overestimation in the modelled

precipitation field. There is good agreement between the model and observations in the regime separation and there are no cases in which the model and observation disagreed on regime diagnosis, but this is in part due to the limited number of observations.

However, one case that did have disagreement occurred at Camborne over 2 and 3 August. On 2 August the model produced a defined timescale but the observations did not and on 3 August the observations had a defined timescale but the model did not. The model and observed timescales for this region are different, in essence due to the different timings of convection.

Events also occurred when precipitation was not observed but the model showed a situation in convective quasi-equilibrium. This is likely to be due to a wrong placement of the convection rather than a timing or intensity issue, and has been previously found for convective quasi-equilibrium conditions (e.g. Done *et al.*, 2006; Keil and Craig, 2011; Done *et al.*, 2012; Keil *et al.*, 2014). Such a situation is illustrated in Figure 2 where the orientation of the convergence line over Cornwall in the radar image (Figure 2(e)) differs from the orientation of the corresponding region of long model-derived convective adjustment timescale (Figure 2(a)). There were also some times when non-equilibrium convection did not occur in the model but did in reality.

In summary, two caveats with the model-derived regimes have been identified:

(i) the model overestimates the precipitation, potentially leading to more convective events than observed and so more convective quasi-equilibrium events than observed; and
(ii) the model can retain CAPE for too long, potentially leading to convective adjustment timescales being overestimated. However, the overall robustness of the model-derived regime separation provides confidence in the use of the model-derived precipitation and CAPE fields for the climatological classification of convection over the British Isles.

4. Model climatology of the convective adjustment timescale over the British Isles

The following aspects of the climatology are analysed in this section: frequency distribution, spatial variation, diurnal cycle, and relationship to the large-scale wind speed and direction.
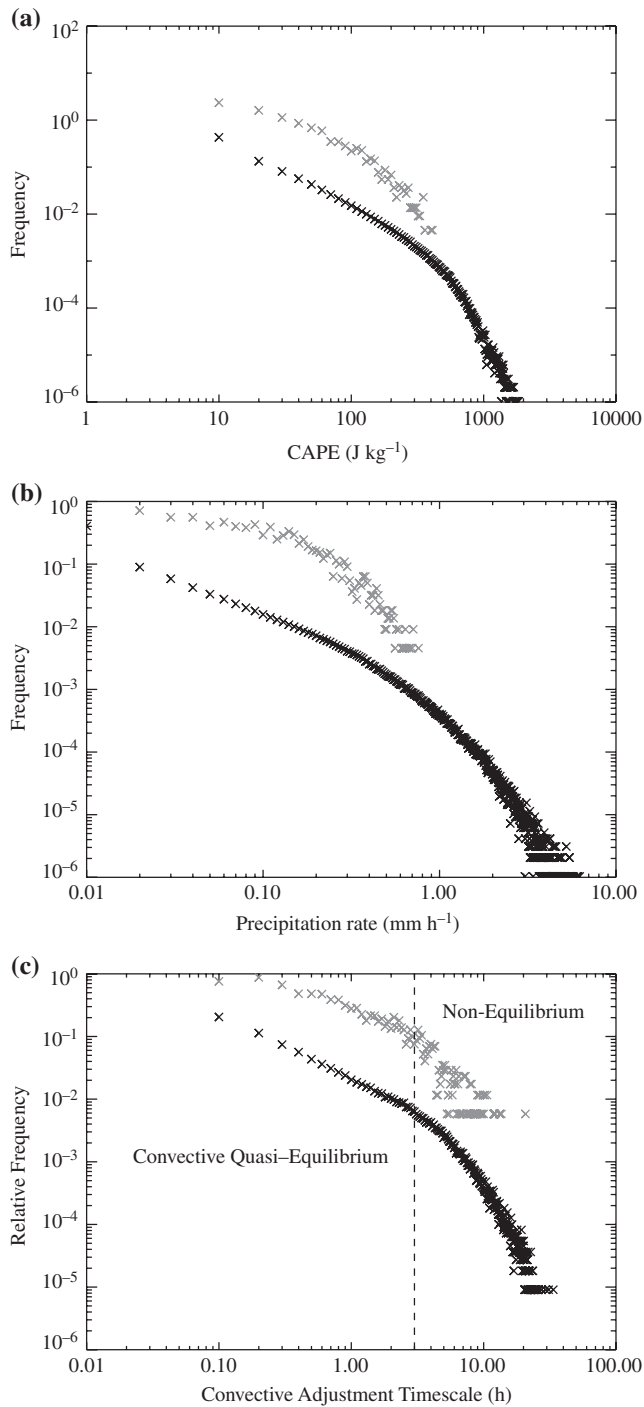
4.1. Frequency distribution of the convective adjustment timescale

Frequency distributions, either averaged over the UKV model domain (grey) or using all coarse-grained points within the UKV domain (black), are presented for the CAPE, precipitation and convective adjustment timescale in Figure 4. (Note that the distributions for the UKV domain average are shown shifted upwards by an order of magnitude to allow easier comparison.) The UKV domain-average distributions (grey) have shallower gradients for small values of the fields and wider distributions towards the larger values of the fields than the distribution using all points in the domain (black). However, the overall structures of the distributions are independent of whether or not the fields are averaged across the domain for all three fields.

Figure 4(a) shows that low values of CAPE (less than $\sim$100 J kg^{-1}) occur most frequently. Such low CAPE values are typically associated with shallow convection (Siebesma, 1998). Large CAPE accumulation is rare. Although the average over the British Isles does not exceed 500 J kg^{-1}, there are locations, such as the southwest peninsula of the UK (Devon and Cornwall), where the local CAPE values can exceed 1000 J kg^{-1} given the right atmospheric conditions (the larger values in the black distribution).

Precipitation (Figure 4(b)) has a similarly shaped frequency distribution curve to that of the CAPE, with a large proportion of light precipitation during the period examined. The distribution

(a)

(b)

(c)

Figure 4. Frequency distributions for the UKV domain showing (a) CAPE, (b) precipitation rate (no thresholding applied) and (c) the convective adjustment timescale (calculated using thresholded precipitation) for JJA 2012–2014 as an average over the coarse-grained UKV model output (grey) and over all coarse-grained points in the domain (black). Bin sizes are 10 J kg^{-1} for CAPE, 0.01 mm h^{-1} for precipitation and 0.1 h for convective adjustment timescale. Frequency is shown normalised by the total number of events–the maximum possible number of events is 92 days × 3 years × 8 time periods per day (UKV domain average) and 92 days × 3 years × 8 time periods per day × 440 grid points (all points in UKV domain), but zero values and undefined values (the timescale is undefined for zero precipitation) are not shown. The distributions for the UKV domain average in each plot have been shifted upwards by an order of magnitude to allow easier comparison.

curve is wider (more variable) than that of the CAPE, which is assumed to be associated with the inherent differences in the characteristics of these fields (CAPE tends to have smoother spatial and temporal variation than precipitation).

The convective adjustment timescale (Figure 4(c)) shows the expected wide distribution curve similar to that of precipitation and has a change in behaviour at around 3 h. This scale break

is particularly evident in the UKV domain-average curve (grey distribution in Figure 4(c)), although there is evidence of it also in the distribution using all points (black distribution in Figure 4(c)). There is a distinct change in the gradient of the distribution curve below and above 3 h, from −1.0 for convective quasi-equilibrium to −2.8 for non-equilibrium convection. This supports the hypothesis of a change in regime occurring dependent on the convective adjustment timescale and the choice of 3 h as the convective adjustment timescale threshold that distinguishes between the two convective regimes. Such a change in gradient was not observed in a frequency distribution of the convective adjustment timescale over Germany (Figure 1 in Zimmer *et al.*, 2011) which had a gradient of −1.3 throughout the distribution. Given the different data sources, the slope of the German data is considered to be consistent with the slope found here for the equilibrium regime in the UK data.

The scale break occurs within the timescales of 3–5 h, based on the fit of a sufficiently straight line to the distribution on each side of the designated break (where a sufficiently straight line is defined as a Pearson's correlation value of at least 0.98). The line slopes obtained within the 3–5 h break point range vary from −1.0 to −1.1 in equilibrium conditions and −2.8 to −3.0 in non-equilibrium conditions. Sensitivity tests were performed to explore whether the change in gradient found here could be an artifact of the method used to calculate the timescale, in particular the use of 3 h precipitation accumulations. The frequency distribution was recalculated using hourly precipitation accumulations for a sample year and also separately for the different years using 3 h precipitation accumulations. The frequency distribution using hourly precipitation accumulations (not shown) has similar gradients for convective adjustment timescales less than and greater than 3 h to those in Figure 4(c). The distributions for the separate years (also not shown) are consistent, with a similar regime split for each year, implying that the break is a robust feature.

Using a threshold of 3 h to distinguish between the convective regimes shows that 85% of the convection occurs in a quasi-equilibrium convective regime and 15% in a non-equilibrium convective regime. This difference is larger than was observed over Germany (Zimmer *et al.*, 2011). Varying the threshold time-scale (Table 1) shows that the regime frequencies for the two countries become comparable if a regime threshold of 1 h is used for the data over the British Isles and 24 h for that over Germany; again this is robust to using a UKV domain average or all points within the domain (Table 1). One possible reason for this disparity is the different data sources used by the two studies: model output for the present study and observations for the Zimmer *et al.* (2011) study. However, the comparison in section 3 provides some confidence in the model-derived timescales. Other possible reasons relate to the different convective environments in each country (i.e. a maritime climate in the British Isles and a continental climate over Germany). For example, the British Isles has smaller precipitation rates (Huffman *et al.*, 1997) and CAPE (Romero *et al.*, 2007; Riemann-Campe *et al.*, 2009) than continental Europe, particularly the central and eastern parts of the continent. The smaller CAPE is associated with a greater

Table 1. Percentage frequency of JJA quasi-equilibrium convective events in the British Isles for both domain-averaged and all points (this study) and Germany (Zimmer *et al.*, 2011). The columns are for different threshold timescales used to distinguish equilibrium and non-equilibrium regimes.

	τ_c (h)				
	<1	<3	<6	<12	<24
British Isles (domain average)	63.3	84.9	95.0	99.2	100.0
British Isles (all points)	63.1	84.8	95.0	99.2	100.0
Germany	31.2	44.9	52.0	59.0	66.6

likelihood of shallow convection forming over the British Isles. To test the hypothesis about the different climates conclusively would required climatologies of the timescale to be calculated for different locations (both maritime and continental) across the globe to see if these regime differences are more general; this is beyond the scope of this article.

Other factors responsible for these differences and the consequent domination of quasi-equilibrium convective conditions over the British Isles are hypothesised to include its topography (with higher elevations to the west over Scotland and Wales (Figure 1)), its position at the end of the extratropical storm track, and land–sea interactions around the coastlines. The roles of coastal influences and topography are considered in the next subsection.

### 4.2. Spatial variation of the convective adjustment timescale

The spatial variations in the coarse-grained three-year JJA climatologies of CAPE, precipitation and convective adjustment timescale across the British Isles and near continent are shown in Figure 5. CAPE is largest in the continental region included in the model domain and in the southwest of the domain (Figure 5(a)). There is a slight meridional CAPE gradient with the highest values in the south; this is linked to the meridional temperature gradient across the UKV domain, due to decreased insolation with increasing latitude. Coarse-grained precipitation varies between 0.05 and 0.25 mm h^{-1} over the domain before application of the precipitation threshold used in the calculation of the convective adjustment timescale (Figure 5(b)). The areas with the heaviest precipitation are to the west of the domain and include regions of elevated orography. Precipitation here will likely have been enhanced due to the seeder–feeder effect (Bader and Roach, 1977). Application of the precipitation threshold removes the correlation with orography from the precipitation field (Figure 5(c)) and implies that many of the events over the elevated orography were associated with weakly precipitating stratiform cloud rather convection.

The spatial variation in the convective adjustment timescale is dominated by the meridional decrease in CAPE resulting in convective adjustment timescales varying from 3 h in the south of the domain down to half an hour in the north of the domain (Figure 5(d)). The timescale is longest along coastal orographic gradients: the south coast of Ireland, the north coast of Devon and Cornwall and over the near continent. There is an eastward decrease in the timescale in the south of the domain (in the direction of the prevailing wind) particularly over the southwest peninsula of the UK, thus supporting the hypothesis that the coast has an influence on the timescale. It is speculated that this decrease may be associated with convective cells which increasingly relax their environment towards convective quasi-equilibrium as they develop within the prevailing large-scale flow. It is notable that regions of elevated orography are not associated with long timescales, implying that non-equilibrium convection does not preferentially occur here. The spatial distribution of the percentage frequency of non-equilibrium convective events (Figure 6) shows that these events preferentially occur in the south and west of the domain, and is broadly consistent with an envelope of the distribution of the average convective adjustment timescale for 1.5 h and above.

4.3. Diurnal cycle of the convective adjustment timescale

Well-documented diurnal cycles exist in the convective precipitation (Yang and Slingo, 2001) and CAPE (Dai *et al.*, 1999), implying the likely existence of a diurnal cycle in the convective adjustment timescale. In summer, CAPE over land often builds up during the day as surface temperatures increase, reaching a peak in early to mid-afternoon after which the instability is released and convection (and precipitation) increases. As CAPE builds up,

the convective adjustment timescale may be expected to increase (assuming relatively constant precipitation). As convection is initiated, the precipitation will begin to control the magnitude of the timescale and a decrease in the timescale will occur as CAPE is released and the precipitation reaches its maximum. Hence, the diurnal cycle of the convective adjustment timescale
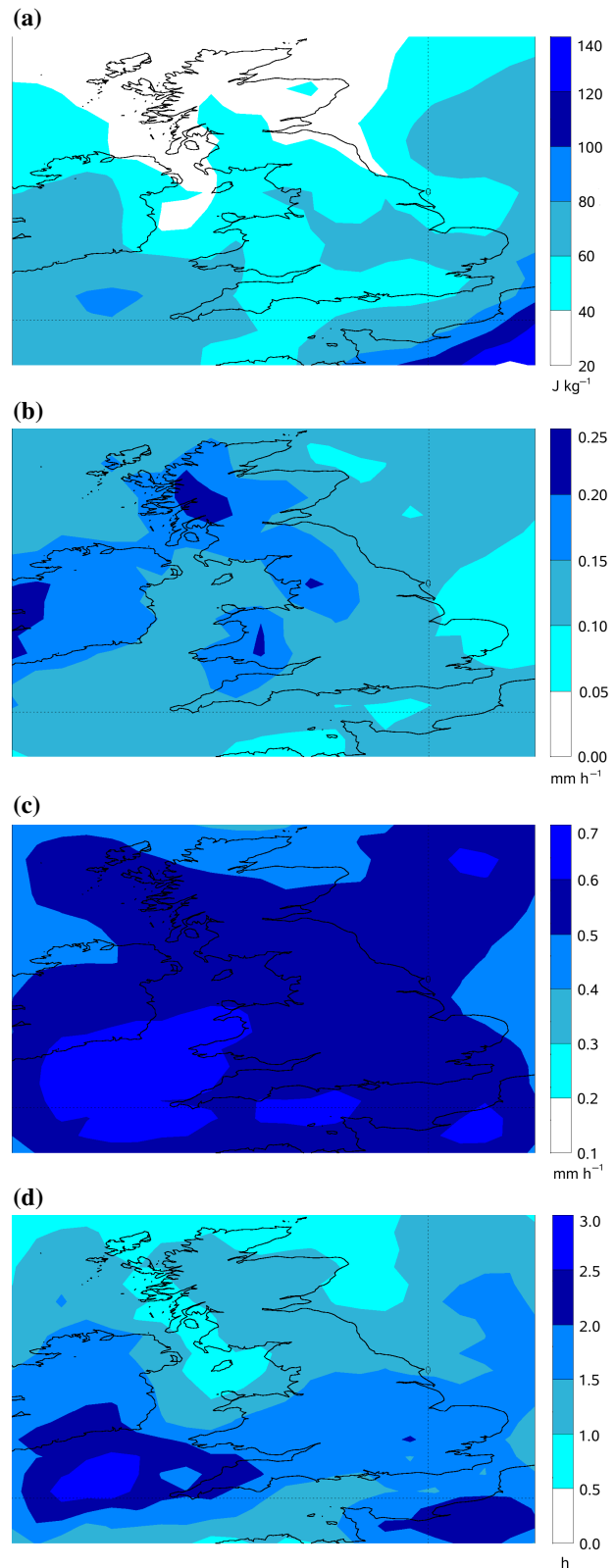
Figure 5. Maps of the coarse-grained UKV domain showing (a) the CAPE, (b) the precipitation rate before the precipitation threshold is applied, (c) the precipitation rate after the threshold has been applied and (d) the convective adjustment timescale. All fields are averages over three-hourly data from JJA 2012–2014 including zero values but excluding undefined convective adjustment timescales.
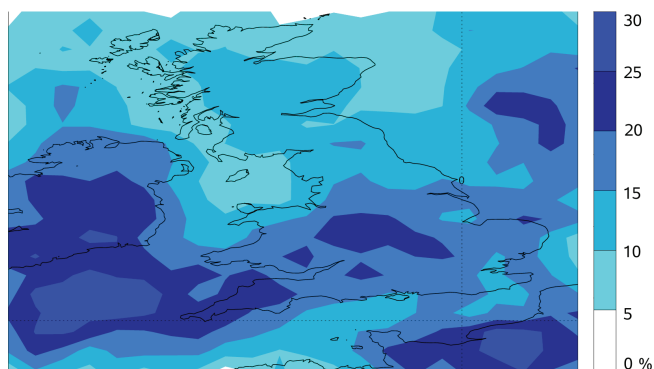
Figure 6. Map of the coarse-grained UKV domain showing the percentage of non-equilibrium events at each gridpoint in the domain.

over land is predicted be approximately in phase with that of the CAPE and to lead that of the precipitation (Keil *et al.*, 2014). The greater heat capacity of the oceans compared to the land results in a weaker diurnal cycle in surface temperature, and hence convection (Hendon and Woodberry, 1993; Bechtold *et al.*, 2004). The diurnal cycle is thus expected to have a reduced amplitude over the oceans.

The diurnal cycles of CAPE, precipitation and convective adjustment timescale over land and sea are shown in Figure 7. The plots show the median and 25th and 75th percentiles of the fields at each time (in box-plot format); the same diurnal cycle behaviours are seen in the extremes of the distributions (not shown). As predicted, the diurnal cycles in all three fields are weak over the sea but marked over the land. Over land, the peak in the diurnal cycle in convective adjustment timescale leads those of CAPE and precipitation by 3 and 6 h respectively. The identification of land and sea points has been taken from a coarse-grained UKV land–sea mask; points with a fractional land value greater than 0.8 have been classed as land, points with a value of less than 0.2 have been classed as sea, and remaining points have been classed as coastal points. The coastal points have a damped diurnal cycle in comparison with the land points (not shown). The diurnal cycle results are robust to the exact definition of land or sea points.

A diurnal cycle in the convective adjustment timescale is also clearly evident in subdaily spatial distributions of the coarse-grained three-year JJA climatology of convective adjustment timescale (shown in Figure 8 for four selected 3 h periods). The timescale has a relatively zonal distribution in the morning, (0900–1200 UTC, equivalent to 1000–1300 BST*, Figure 8(a)). It peaks in southwest England in the early afternoon (Figure 8(b)), eastern England in late afternoon (Figure 8(c)) and over the southwest sea approaches to England overnight (Figure 8(d)).

4.4. Relationship between the convective adjustment timescale and the synoptic-scale wind field

Winds were considered at a hybrid-model-level height of 1.4 km, chosen to give an indication of the storm motion and as being typically near the top of, or above, the boundary layer. Figure 9 shows variants of a wind rose, with the incremental radius of the segments indicating the percentage frequency of different convective adjustment timescale bands, from all coarse-grained points within four different regions across the British Isles (marked on Figure 1). The percentages written at the boundaries of the panels refer to the frequency with which the wind is from the particular sector. Therefore, the difference between the sum of the percentages plotted and that written for a given sector represents the percentage frequency for which the timescale is

undefined (i.e. no convective precipitation occurring). Other regions across the British Isles were also considered and it was found that the results shown in Figure 9 are robust and provide a good description of spatial variation across the British Isles. These particular regions were chosen as they included a range of surface types: mainly ocean (the North Sea region, Figure 9(a)), coastal with elevated cliffs and islands (western Scotland, Figure 9(b)), large orographic coastal gradients and in the south (southwest England, Figure 9(c)), and close to the continent and mainly land (southeast England, Figure 9(d)). All regions show some convective events for every wind direction but are dominated by westerly to southerly sectors, as in Hand (2005). Non-equilibrium convection (convective adjustment timescale exceeding 3 h) occurs most frequently when the wind directions are westerly to southerly, indicating that CAPE is most likely to build under these conditions. The four different regions include differing proportions of land and sea. The general consistency between the wind roses shown suggests that coastal effects (such as sea breezes) do not have a dominant effect on the convective adjustment timescale.

Some patterns emerge from comparing the different wind roses. The percentage occurrence of winds from the westerly and southwesterly sectors decreases when comparing more easterly with more westerly regions (Figure 9(b, d) with Figure 9(a, c) respectively) and comparing more northerly with more southerly (Figure 9(a, b) with Figure 9(c, d)). The frequency for which the convective adjustment timescale is undefined (implying precipitation rates below the threshold at all coarse-grained grid points in that region) is greater in the eastward regions than in the westward regions, associated with the eastward decline in climatological precipitation. The frequency associated with non-equilibrium convection is greatest in the southwest region (Figure 9(c), consistent with Figure 5(d)). Thus, the frequency that longer convective adjustment timescale are diagnosed decreases in the direction of the prevailing winds. This suggests that the convective environment relaxes towards quasi-equilibrium as systems move away from triggering locations in the southwest.

Figure 10 is plotted in the same format as Figure 9. Here the data from the southwest region are shown separately for three different wind speed ranges. When the winds are strong ($>15\,\mathrm{m\,s^{-1}}$) they are southwesterly or westerly about 85% of the time, whereas when the winds are weak ($<5\,\mathrm{m\,s^{-1}}$) there is a slight preference for southwesterly or westerly winds. There is limited convection at weak wind speeds (hence the timescale is rarely defined in Figure 10(a)), and as the wind speed increases the frequency of convection increases. The strongest wind speeds (Figure 10(c)) are dominated by convective quasi-equilibrium events, perhaps due to the reduced effects of local influences and the reduced likelihood of local circulations. For example, sea breezes do not form in strong synoptic-scale winds (e.g. Estoque, 1962; Bechtold *et al.*, 1991; Zhong and Takle, 1993) and hence convection situated along a sea-breeze front cannot form. Most of the non-equilibrium convection occurs within the intermediate wind speed regime (5–$15\,\mathrm{m\,s^{-1}}$) which happens 64.2% of the time, for which the winds are not too strong to suppress mesoscale circulations.

5. Summary

Convection-permitting modelling has undoubtedly led to a step change in the forecasting of convective precipitation (e.g. Lean *et al.*, 2008). However many aspects of forecasting with such models are not yet well understood, the variation in predictability characteristics for convective events being one good example. The convective adjustment timescale provides a useful predictability-relevant measure of the environmental conditions within which a convective event occurs. This study has used that timescale to characterise the weather regimes associated with convection

---

*British Summer Time.
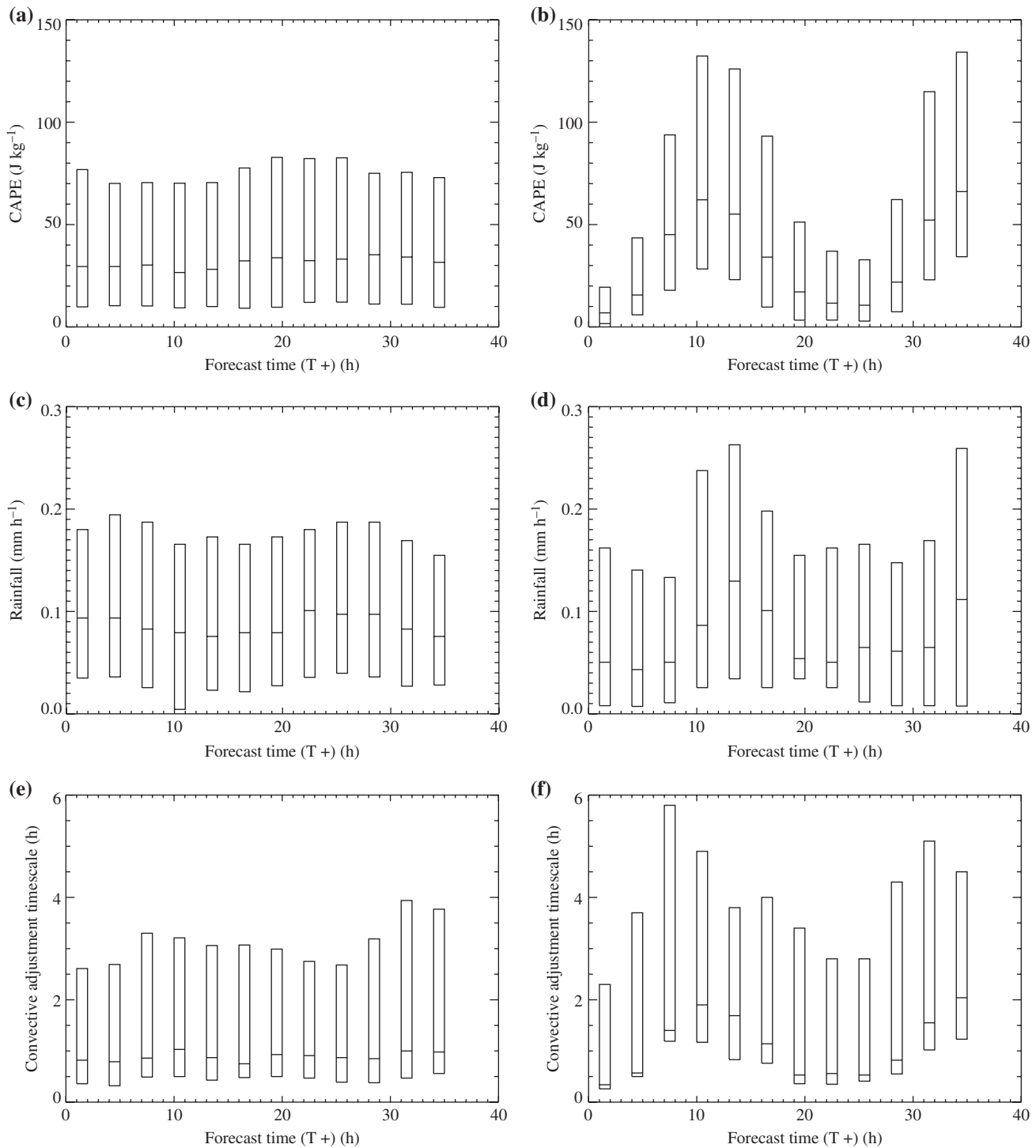
Figure 7. Box plots of spatially averaged (a) CAPE over the sea, (b) CAPE over the land, (c) precipitation over the sea, (d) precipitation over the land, (e) the convective adjustment timescale over the sea and (f) the convective adjustment timescale over the land, as functions of forecast time for JJA 2012−2014. The plots are constructed from 3 h averages from the analysis time such that the first box represents T+0 to T+3 (0300−0600 UTC), etc. The boxes represent the interquartile range and the line within the box represents the median.

over the British Isles, distinguishing between convective quasi-equilibrium and non-equilibrium, and has had a particular focus on the spatial, temporal and flow-dependent nature of the timescale. For this purpose, operational output from the UKV configuration of the MetUM was coarse-grained to compute the convective adjustment timescale over three summers (JJA 2012−2014). The model-derived results were shown to be consistent with observations. Moreover, a comparison of the three years within the model output indicated a consistent split between the regimes for each year.

It was shown that the British Isles is more frequently in a convective quasi-equilibrium regime than Germany; 85% of the convection in the British Isles was categorised in convective

quasi-equilibrium, compared to 66% in Germany (Zimmer *et al.*, 2011). Unlike the German frequency distribution, there was a distinct change in gradient (i.e. a scale break) in the British Isles frequency distribution between the two regimes. This is hypothesised to be because of the maritime climate, though further testing in different regions of the globe would be required to confirm this.

A threshold timescale was set that was consistent with the change in gradient. The convective adjustment timescale was examined at different times of day and was shown to have a diurnal cycle that was linked with those for CAPE and precipitation (Figure 7). The diurnal cycle over land is clearer than that offshore, in line with previous work (e.g. Hendon and Woodberry, 1993).

(a)

(b)

(c)

(d)
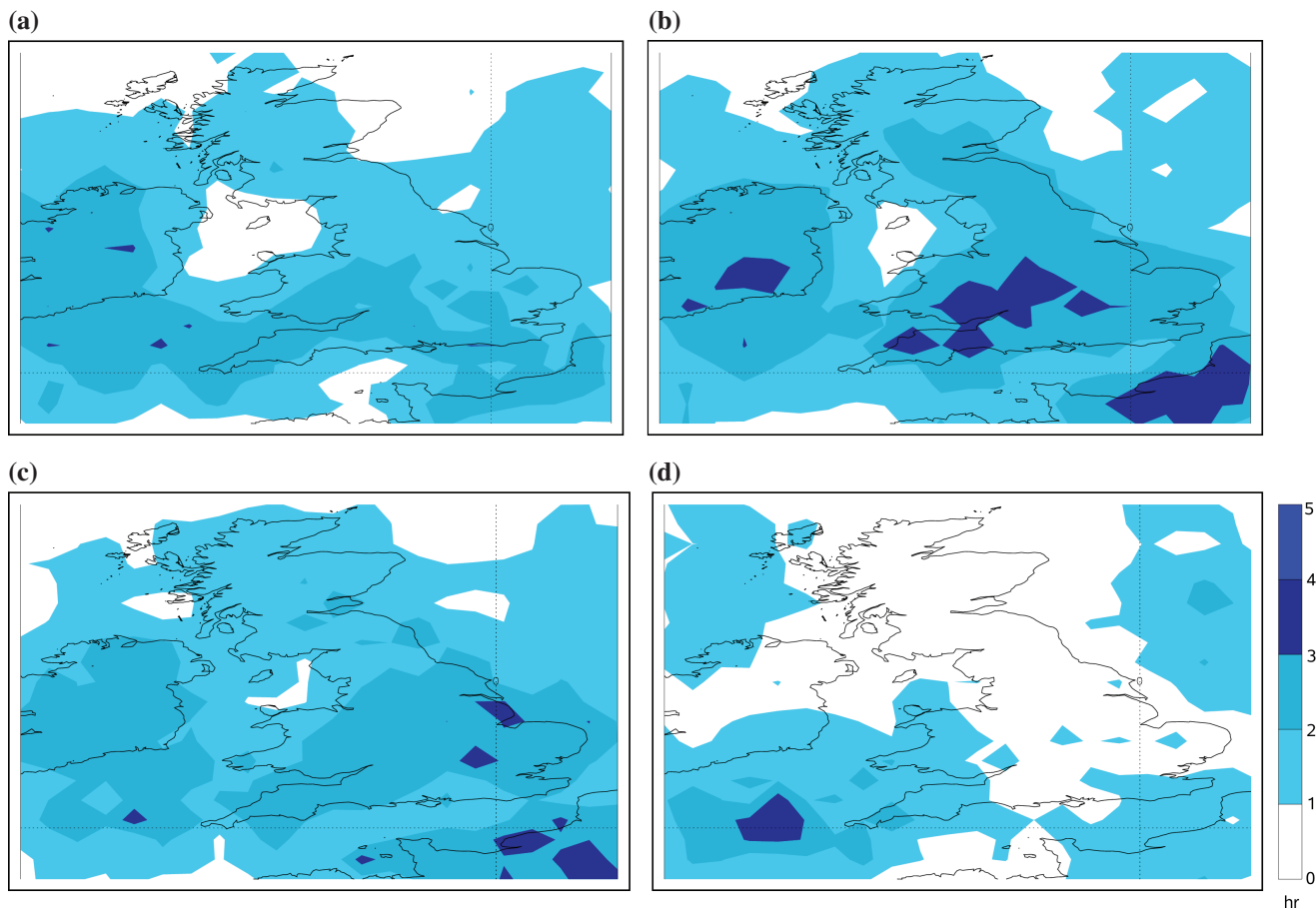
Figure 8. The average convective adjustment timescale for JJA 2012−2014 at (a) T+6 to T+9 (0900−1200 UTC), (b) T+9 to T+12 (1200−1500 UTC), (c) T+12 to T+15 (1500−1800 UTC) and (d) T+18 to T+21 (2100−0000 UTC). The colour scale refers to all plots.
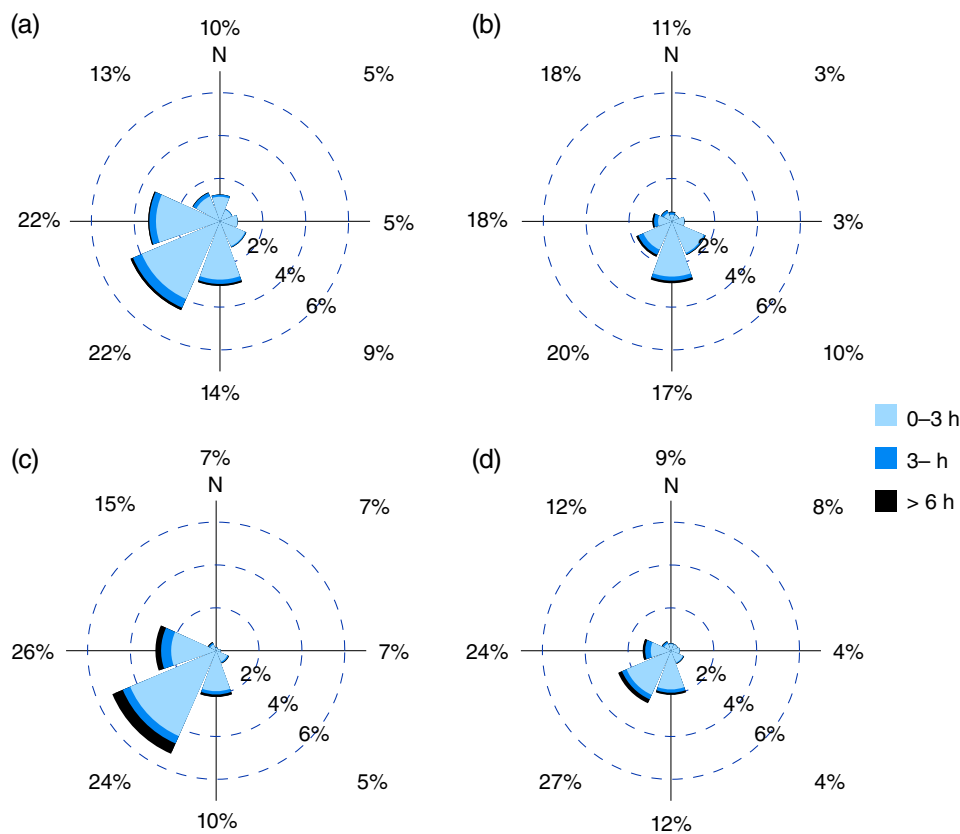
Figure 9. A wind rose variant, where the concentric rings show the frequency of the wind direction and the colours mark the magnitude of the convective adjustment timescale over the period JJA 2012−2014 using T+6 to T+30 h coarse-grained UKV model output averaged over the regions (a) western Scotland, (b) the North Sea, (c) the southwest and (d) the southeast of the UK. The regions are marked in Figure 1 and the colour scale refers to all plots. The percentages on the edge of the panels show how often the wind comes from that direction in total.
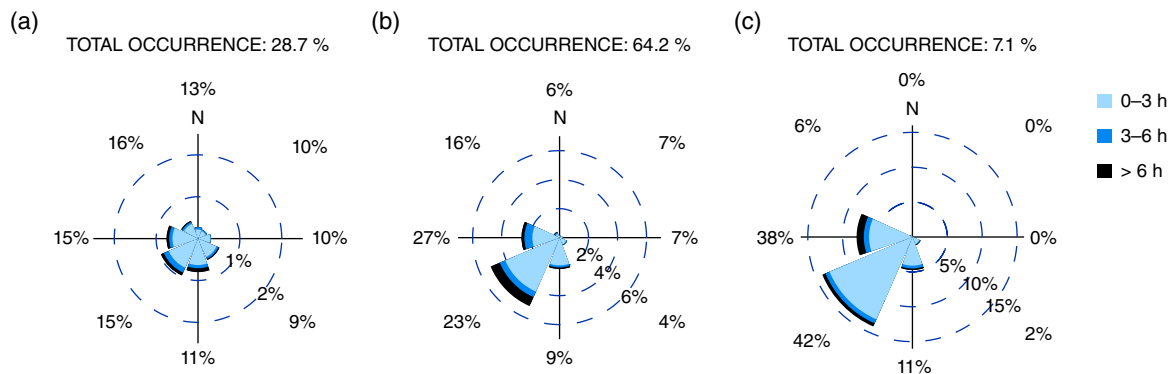
Figure 10. Convective adjustment timescale rose for the southwest region as a percentage of the time that the wind is in each sector and for wind speeds (a) $0-5\,\mathrm{m\,s^{-1}}$, (b) $5-15\,\mathrm{m\,s^{-1}}$, and (c) $>15\,\mathrm{m\,s^{-1}}$. The frequency of occurrence for each wind speed is shown above the relevant wind rose. The colour scale refers to all plots. The percentages on the edge of the panels show how often the wind comes from that direction. Note that a different scale is used for (a).

As in Keil and Craig (2011) and Keil *et al.* (2014), there was evidence that the evolution of convective systems has an impact on the timescale diagnosed, here considered in terms of position of the convective cells. Specifically, it was found that there is a distinct track running from the southwest to the northeast along which the timescale was shown to decay. Although this result is consistent with the climatological flow, convective events in the British Isles can also develop downstream of events that form initially over the European continent and as such the regime categorisation could depend on the direction of the synoptic-scale wind. It was shown that most convective events over the British Isles are associated with westerly to southwesterly flow as in Hand (2005), but at all wind speeds non-equilibrium events are more likely to be associated with wind directions that are downstream of the continent or else downstream of large orographic gradients (Figure 9).

The wind speed was also found to have some influence over the regime classification, with non-equilibrium convection mainly occurring for intermediate wind speeds between 5 and 15 m s^{-1}. In the weakest wind regime convection was rare, while strong winds are more likely to suppress mesoscale or small-scale circulations, such as sea breezes (Estoque, 1962), that could act as local mechanisms to initiate non-equilibrium convection.

This study has characterised convective regimes over the British Isles, and is intended to inform and provide a context for future study of convective-scale error growth for convection-permitting forecasting within this region. A limitation of the study is that the use of a precipitation threshold on accumulations could have led to some stratiform rain being included within the calculation of the timescale, particularly over mountainous regions where the seeder–feeder mechanism can act to enhance precipitation. However, convective precipitation is difficult to identify unambiguously and the same limitation is also present in other studies to have considered this timescale. To reduce this effect the most intense 17% of the coarse-grained precipitation was considered here.

There are many implications of this work for forecasting convection within the British Isles. For example, with convective quasi-equilibrium conditions dominating convection within the British Isles, it is likely that more reliable forecasts for this type of convection will place relatively more emphasis on the use of large-member ensembles as opposed to higher-resolution models. Furthermore, given the link of the regimes to the large-scale wind field, the results could be used to help design an adaptive ensemble forecasting system for the British Isles.

Acknowledgements

References

Arakawa A, Schubert WH. 1974. Interaction of a cumulus cloud ensemble with the large-scale environment, part I. *J. Atmos. Sci.* **31**: 674–701, doi: 10.1175/1520-0469(1974)031<0674:ioacce>2.0.CO;2.

Bader M, Roach W. 1977. Orographic rainfall in warm sectors of depressions. *Q. J. R. Meteorol. Soc.* **103**: 269–280, doi: 10.1002/qj.49710343605.

Baldauf M, Seifert A, Förstner J, Majewski D, Raschendorfer M, Reinhardt T. 2011. Operational convective-scale numerical weather prediction with the COSMO model: Description and sensitivities. *Mon. Weather Rev.* **139**: 3887–3905, doi: 10.1175/MWR-D-10-05013.1.

Bechtold P, Pinty JP, Mascart F. 1991. A numerical investigation of the influence of large-scale winds on sea-breeze-and inland-breeze-type circulations. *J. Appl. Meteorol.* **30**: 1268–1279, doi: 10.1175/1520-0450(1991)030<1268:anioti>2.0.CO;2.

Bechtold P, Chaboureau JP, Beljaars A, Betts A, Köhler M, Miller M, Redelsperger JL. 2004. The simulation of the diurnal cycle of convective precipitation over land in a global model. *Q. J. R. Meteorol. Soc.* **130**: 3119–3137, doi: 10.1256/qj.03.103.

Bennett LJ, Browning KA, Blyth AM, Parker DJ, Clark PA. 2006. A review of the initiation of precipitating convection in the United Kingdom *Q. J. R. Meteorol. Soc.* **132**: 1001–1020, doi: 10.1256/qj.05.54.

Best MJ, Pryor M, Clark DB, Rooney GG, Essery RL, Ménard CB, Edwards JM, Hendry MA, Porson A, Gedney N, Mercado LM, Sitch S, Blyth E, Boucher O, Cox PM, Grimmond CSB, Harding RJ. 2011. The Joint UK Land Environment Simulator (JULES), model description, part 1: Energy and water fluxes. *Geosci. Model Dev.* **4**: 677–699, doi: 0.5194/gmd-4-677-2011.

Burt S. 2005. Cloudburst upon Hendraburnick Down: The Boscastle storm of 16 August 2004. *Weather* **60**: 219–227, doi: 10.1256/wea.26.05.

Craig GC, Dörnbrack A. 2008. Entrainment in cumulus clouds: What resolution is cloud-resolving? *J. Atmos. Sci.* **65**: 3978–3988, doi: 10.1175/2008JAS2613.1.

Craig GC, Keil C, Leuenberger D. 2012. Constraints on the impact of radar rainfall data assimilation on forecasts of cumulus convection. *Q. J. R. Meteorol. Soc.* **138**: 340–352, doi: 10.1002/qj.929.

Dai A, Giorgi F, Trenberth KE. 1999. Observed and model-simulated diurnal cycles of precipitation over the contiguous United States. *J. Geophys. Res.* **104**: 6377–6402, doi: 10.1029/98JD02720.

Davies T, Cullen MJP, Malcolm A, Mawson M, Staniforth A, White AA, Wood N. 2005. A new dynamical core for the Met Office's global and regional modelling of the atmosphere. *Q. J. R. Meteorol. Soc.* **131**: 1759–1782, doi: 10.1256/qj.04.101.

Done J, Craig GC, Gray SL, Clark PA, Gray M. 2006. Mesoscale simulations of organized convection: Importance of convective equilibrium. *Q. J. R. Meteorol. Soc.* **132**: 737–756, doi: 10.1256/qj.04.84.

Done J, Craig GC, Gray SL, Clark PA. 2012. Case-to-case variability of predictability of deep convection in a mesoscale model. *Q. J. R. Meteorol. Soc.* **138**: 638–648, doi: 10.1002/qj.943.

Edwards J, Slingo A. 1996. Studies with a flexible new radiation code. I: Choosing a configuration for a large-scale model. *Q. J. R. Meteorol. Soc.* **122**: 689–719, doi: 10.1002/qj.49712253107.

Emanuel KA. 1994. *Atmospheric Convection*. Oxford University Press: Oxford, UK.

Estoque MA. 1962. The sea breeze as a function of the prevailing synoptic situation. *J. Atmos. Sci.* **19**: 244–250, doi: 10.1175/1520-0469(1962)019<0244:tsbaaf>2.0.CO;2.

Glinton M. 2013. 'The role of conditional symmetric instability in numerical weather prediction', PhD thesis. Univeristy of Reading: Reading, UK.

Golding B, Clark PA, May B. 2005. The Boscastle flood: Meteorological analysis of the conditions leading to flooding on 16 August 2004. *Weather* **60**: 230–235, doi: 10.1256/wea.71.05.

Gregory D, Rowntree P. 1990. A mass flux convection scheme with representation of cloud ensemble characteristics and stability-dependent closure. *Mon. Weather Rev.* **118**: 1483–1506, doi: 10.1175/1520-0493(1990)118<1483:amfcsw>2.0.CO;2.

Hand WH. 2005. Climatology of shower frequency in the British Isles at 5 km resolution. *Weather* **60**: 153–158, doi: 10.1256/wea.129.04.

Hand WH, Fox NI, Collier CG. 2004. A study of twentieth-century extreme rainfall events in the United Kingdom with implications for forecasting. *Meteorol. Appl.* **11**: 15–31, doi: 10.1017/S1350482703001117.

Hanley K, Plant R, Stein T, Hogan R, Lean HW, Halliwell C, Clark PA. 2014. Mixing-length controls on high-resolution simulations of convective storms. *Q. J. R. Meteorol. Soc.* **141**: 272–284, doi: 10.1002/qj.2356.

Hendon HH, Woodberry K. 1993. The diurnal cycle of tropical convection. *J. Geophys. Res.* **98**: 16623–16637, doi: 10.1029/93JD00525.

Huffman GJ, Adler RF, Arkin P, Chang A, Ferraro R, Gruber A, Janowiak J, McNab A, Rudolf B, Schneider U. 1997. The Global Precipitation Climatology Project (GPCP) combined precipitation dataset. *Bull. Am. Meteorol. Soc.* **78**: 5–20, doi: 10.1175/1520-0477(1997)078<0005:tgpcpg>2.0.CO;2.

Keil C, Craig GC. 2011. Regime-dependent forecast uncertainty of convective precipitation. *Meteorol. Z.* **20**: 145–151.

Keil C, Heinlein F, Craig GC. 2014. The convective adjustment times-scale as indicator of predictability of convective precipitation. *Q. J. R. Meteorol. Soc.* **140**: 480–490, doi: 10.1002/qj.2143.

Kober K, Craig GC, Keil C. 2014. Aspects of short-term probabilistic blending in different weather regimes. *Q. J. R. Meteorol. Soc.* **140**: 1179–1188, doi: 10.1002/qj.2220.

Kühnlein C, Keil C, Craig GC, Gebhardt C. 2014. The impact of downscaled initial condition perturbations on convective-scale ensemble forecasts of precipitation. *Q. J. R. Meteorol. Soc.* **140**: 1552–1652, doi: 10.1002/qj.2238.

Lean HW, Clark PA, Dixon M, Roberts NM, Fitch A, Forbes R, Halliwell C. 2008. Characteristics of high-resolution versions of the Met Office Unified Model for forecasting convection over the United Kingdom. *Mon. Weather Rev.* **136**: 3408–3424, doi: 10.1175/2008MWR2332.1.

Leon DC, French JR, Lasher-Trapp S, Blyth AM, Abel SJ, Ballard SP, Barrett A, Bennett LJ, Bower K, Brooks B, Brown P, Charlton-Perez C, Choularton T, Clark PA, Collier C, Crosier J, Cui Z, Dey S, Dufton D, Eagle C, Flynn MJ, Gallagher M, Halliwell C, Hanley K, Hawkness-Smith L, Huang Y, Kelly G, Kitchen M, Korolev A, Lean HW, Liu Z, Marsham J, Moser D, Nicol J, Norton EG, Plummer D, Price J, Ricketts H, Roberts NM, Rosenberg PD, Simonin D, Taylor JW, Warren R, Williams PI, Young G. 2015. The COnvective Precipitation Experiment (COPE): Investigating the origins of heavy precipitation in the southwestern UK. *Bull. Am. Meteorol. Soc.*, doi: 10.1175/BAMS-D-14-00157.1.

Lewis MW, Gray SL. 2010. Categorisation of synoptic environments associated with mesoscale convective systems over the UK. *Atmos. Res.* **97**: 194–213, doi: 10.1016/j.atmosres.2010.04.001.

Lock AP, Brown A, Bush M, Martin G, Smith R. 2000. A new boundary-layer mixing scheme. Part I: Scheme description and single-column model tests. *Mon. Weather Rev.* **128**: 3187–3199, doi: 10.1175/1520-0493(2000)128<3187:anblms>2.0.CO;2.

Lorenz EN. 1969. The predictability of a flow which possesses many scales of motion. *Tellus* **21**: 289–307, doi: 10.1111/j.2153-3490.1969.tb00444.x.

Met Office. 2003. 1 km Resolution UK Composite Rainfall Daata from the Met Office Nimrod System. NCAS British Atmospheric Data Centre: Harwell, UK. http://catalogue.ceda. ac.uk/uuid/27dd6ffba67f667a18c62de5c3456350 (accessed 16 February 2016).

Met Office. 2006. Met Office Global Radiosonde Data. NCAS British Atmospheric Data Centre: Harwell, UK. http://catalogue.ceda.ac.uk/uuid/f2afaf808b61394b78bd342ff068c8cd (accessed 16 February 2016).

Met Office. 2012a. Met Office Integrated Data Archive System (MIDAS) Land and Marine Surface Stations Data (1853–current). NCAS British Atmospheric Data Centre: Harwell, UK. http://catalogue.ceda.ac.uk/uuid/220a65615218d5c9cc9e4785a3234bd0 (accessed 16 February 2016).

Met Office. 2012b. Summer 2012. http://www.metoffice.gov.uk/ climate/uk/summaries/2012/summer (accessed 16 February 2016).

Met Office. 2013. Summer 2013. http://www.metoffice.gov.uk/ climate/uk/summaries/2013/summer (accessed 16 February 2016).

Met Office. 2014. Summer 2014. http://www.metoffice.gov.uk/ climate/uk/summaries/2014/summer (accessed 16 February 2016).

Mittermaier MP. 2014. A strategy for verifying near-convection-resolving model forecasts at observing sites. *Weather and Forecasting* **29**: 185–204, doi: 10.1175/WAF-D-12-00075.1.

Mittermaier MP, Roberts N, Thompson SA. 2013. A long-term assessment of precipitation forecast skill using the Fractions Skill Score. *Meteorol. Appl.* **20**: 176–186, doi: 10.1002/met.296.

Molini L, Parodi A, Rebora N, Craig GC. 2011. Classifying severe rainfall events over Italy by hydrometeorological and dynamical criteria. *Q. J. R. Meteorol. Soc.* **137**: 148–154, doi: 10.1002/qj.741.

Riemann-Campe K, Fraedrich K, Lunkeit F. 2009. Global climatology of Convective Available Potential Energy (CAPE) and Convective Inhibition (CIN) in ERA-40 reanalysis. *Atmos. Res.* **93**: 534–545, doi: 10.1016/j.atmosres.2008.09.037.

Romero R, Gayà M, Doswell CA III. 2007. European climatology of severe convective storm environmental parameters: A test for significant tornado events. *Atmos. Res.* **83**: 389–404, doi: 10.1016/j.atmosres.2005.06.011.

Seity Y, Brousseau P, Malardel S, Hello G, Bénard P, Bouttier F, Lac C, Masson V. 2011. The AROME–France convective-scale operational model. *Mon. Weather Rev.* **139**: 976–991, doi: 10.1175/2010MWR3425.1.

Siebesma AP. 1998. Shallow cumulus convection. In *Buoyant Convection in Geophysical Flows*, NATO ASI Series. Plate EJ, Fedorovich EE, Viegas DX, Wyngaard JC. (eds.), 513: 441–486. Springer: Berlin, doi: 10.1007/978-94-011-5058-3_19.

Stein TH, Hogan RJ, Clark PA, Halliwell CE, Hanley KE, Lean HW, Nicol JC, Plant RS. 2015. The DYMECS project: A statistical approach for the evaluation of convective storms in high-resolution NWP models. *Bull. Am. Meteorol. Soc.* **96**: 939–951, doi: 10.1175/BAMS-D-13-00279.1.

Tang Y, Lean HW, Bornemann J. 2013. The benefits of the Met Office variable-resolution NWP model for forecasting convection. *Meteorol. Appl.* **20**: 417–426, doi: 10.1002/met.1300.

Warren RA, Kirshbaum DJ, Plant RS, Lean HW. 2014. A 'Boscastle-type' quasi-stationary convective system over the UK southwest peninsula. *Q. J. R. Meteorol. Soc.* **140**: 240–257, doi: 10.1002/qj.2124.

Weckwerth TM, Parsons DB. 2006. A review of convection initiation and motivation for IHOP_2002. *Mon. Weather Rev.* **134**: 5–22, doi: 10.1175/MWR3067.1.

Wilson DR, Ballard SP. 1999. A microphysically based precipitation scheme for the UK Meteorological Office Unified Model. *Q. J. R. Meteorol. Soc.* **125**: 1607–1636, doi: 10.1002/qj.49712555707.

Yang GY, Slingo JM. 2001. The diurnal cycle in the tropics. *Mon. Weather Rev.* **129**: 784–801, doi: 10.1175/1520-0493(2001)129<0784:tdcitt>2.0.CO;2.

Yano JI, Plant RS. 2012. Convective quasi-equilibrium. *Rev. Geophys.* 50: RG4004, doi: 10.1029/2011RG000378.

Zhong S, Takle ES. 1993. The effects of large-scale winds on the sea-land-breeze circulations in an area of complex coastal heating. *J. Appl. Meteorol.* **32**: 1181–1195, doi: 10.1175/1520-0450(1993)032<1181:teolsw>2.0.CO;2.

Zimmer M, Craig GC, Keil C, Wernli H. 2011. Classification of precipitation events with a convective response timescale and their forecasting characteristics. *Geophys. Res. Lett.* 38: L05802, doi: 10.1029/2010GL046199.